Orientational dynamics of the glass forming liquid, dibutylphthalate: Time domain experiments and comparison to mode coupling theory

David D. Brace, S. D. Gottke, H. Cang, and M. D. Fayer
Department of Chemistry, Stanford University, Stanford, California 94305

(Received 24 July 2001; accepted 23 October 2001)

Orientation dynamics of the glass forming liquid, dibutylphthalate (DBP), were studied using optical heterodyne detected optical Kerr effect (OHD-OKE) techniques. A combination of experimental methods permitted acquisition of data over 6 decades of time and 5 decades in signal amplitude. Data collected from several hundred fs to several hundred ns, cover the full range of orientational dynamics. The data are compared to the predictions of ideal mode-coupling theory (MCT). Two of the MCT scaling law predictions yield an average value of 227 K for the MCT critical temperature, T_c. Measurements were made at temperatures below T_c. The data were found to agree well with some of the predictions of MCT. The long time scale structural relaxation (α relaxation) obeys the MCT scaling law, and the slowest time scale power law (the von Schweidler power law) is also in accord with MCT predictions. However, the ''master curves'' predicted by MCT fit the data well only at higher temperatures. The master curves show increasingly significant deviations at shorter times ($<$100 ps) as the temperature is decreased, in contrast to previous OHD-OKE studies on salol [G. Hinze, D. D. Brace, S. D. Gottke, and M. D. Fayer, J. Chem. Phys. **113**, 3723 (2000)] and ortho-terphenyl [S. D. Gottke, G. Hinze, D. D. Brace, and M. D. Fayer, J. Phys. Chem. B **105**, 238 (2000)] in which the agreement with ideal MCT is far superior. The DBP data show no discontinuity in the trends as the temperature is reduced below T_c, but an increasingly prominent peak appears in the data at ~2.5 ps. The peak may be related to the boson peak. © *2002 American Institute of Physics.* [DOI: 10.1063/1.1427711]

I. INTRODUCTION

Glass forming materials have the ability to supercool, that is, they can be cooled below the thermodynamic melting point without the onset of crystallization. Glasses are formed when a supercooled liquid (SCL) is cooled sufficiently below the melting point to the glass transition temperature, T_g. Glasses and their associated supercooled liquids occur commonly as natural systems, and they have numerous practical applications. The properties of glasses are determined to a significant extent by the conditions under which they are cooled. Therefore, the dynamics of SCLs, in addition to being of fundamental interest, are important for understanding the properties of glassy materials.

The structural relaxation dynamics of SCLs span an increasingly broad range of times as they are cooled. The slowing down of SCL structural relaxation with decreasing temperature is reflected in microscopic properties, such as orientational relaxation[1–5] and density fluctuations,[6] as well as macroscopic observables like viscosity[7] and long time diffusion.[8] A prominent feature of supercooled liquids is the division of relaxation dynamics into two regions upon cooling. The very fast region, often referred to as the critical decay region (fast β process),[9,10] is usually only mildly temperature dependent. The slower region, often referred to as the α-relaxation region, is strongly temperature dependent. Between the critical decay region and the long time scale α-relaxation region, the dynamics have a complex functional form.[11]

Mode coupling theory (MCT) (Refs. 6, 9) has been utilized to describe SCL dynamics from the picosecond time scale to time scales representing complete structural relaxation (α relaxation). The apparent efficacy of MCT in quantitatively treating the dynamics of SCLs has been the focus of many dynamic light scattering,[9,12–17] neutron scattering,[18–21] dielectric spectroscopy,[19–25] and optical Kerr effect[1,26] experiments as well as computer simulations.[27–30] The above experimental work is comprised of both frequency domain and time domain measurements, which can yield the same information. In practice, however, different dynamical features of a liquid can be emphasized when data are acquired with different methods. Properly conducted time domain can be advantageous for comparisons to the predictions of MCT.[31]

In the present work, heterodyne detected optical Kerr effect (HD-OKE) experiments[31–34] on the glass forming liquid dibutylphthalate (DBP) are presented and compared to the predictions of MCT. (See the inset in Fig. 1 for the molecular structure of DBP.) DBP is a moderately fragile ($m \approx 69$) (Ref. 35) glass former with a melting temperature $T_m = 238$ K and a glass transition temperature $T_g \cong 170$ K. By comparison, Salol is less fragile ($m \approx 63$) (Ref. 35) than DBP, and ortho-terphenyl (OTP) more fragile ($m \approx 76$) (Ref. 35) than DBP. Experiments are conducted that span a range of times from hundreds of fs to several hundred ns. These time scales span the full range of orientational relaxation dynamics. The experiments are conducted from temperatures above the melting point to temperatures below the MCT critical temperature, T_c.

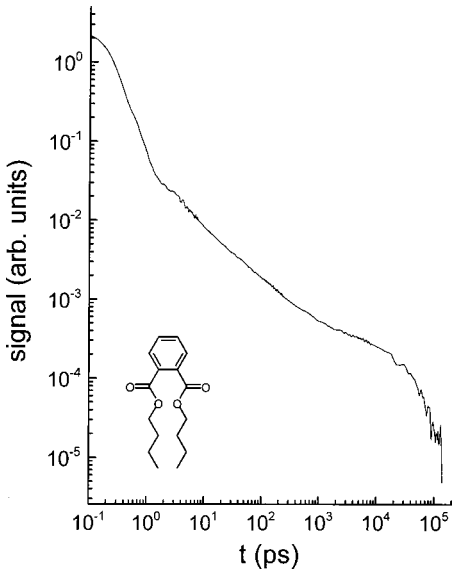

FIG. 1. Optical heterodyne detected optical Kerr effect data taken on supercooled dibutylphthalate at 234.0 K. The data are displayed on a log plot. The data span ~5 decades in amplitude and 6 decades in time from 100 fs to 100 ns. The data decay approximately as an exponential at long time. At shorter times, two regions that decay as power laws can be identified. The inset shows a molecular diagram of dibutylphthalate.

The experiments show good agreement with the predictions of MCT on the time scale of the α relaxation and on the faster time scale of the von Schweidler power law.[6,9] The MCT master curve[36] agrees well with the data only at the highest temperatures. As the temperature is decreased, increasingly large deviations between the data and the master curve occur on times <100 ps. On time scales <100 ps, the master curve predicts decays that are substantially to steep, in contrast to previous work on salol[1] and OTP.[11] While the data do not agree well with MCT on the shorter time scales, it was found that on times short compared to the von Schweidler regime, the data can be described by a temperature independent power law. It is also found that there is no discontinuity in the nature of the decays as the temperature is reduced below T_c. However, as the temperature is decreased below T_c, an increasingly prominent peak appears in the data at ~2.5 ps. This peak may be related to the boson peak.[37]

II. EXPERIMENTAL PROCEDURES

The optical heterodyne detected optical Kerr effect (OHD-OKE), a nonresonant pump–probe experiment,[32,33] measures the time derivative of the polarizability–polarizability correlation function (orientational relaxation).[38,39] The pump pulse induces an optical anisotropy. The induced optical anisotropy decays because of orientational relaxation. The time delayed probe pulse measures the decay. When sufficiently short (≤90 fs) excitation pulses are used, the correspondingly large bandwidth induces an orientationally anisotropic distribution of librations via stimulated Raman scattering. The damping of the optically excited librations leaves behind a residual molecular orientational alignment. When pulses are longer, the corresponding bandwidth is insufficiently broad to initiate librational motions by stimulated Raman scattering. The **E** field associated with longer pulses exerts a torque on molecules with a polarizability anisotropy, which results in a molecular orientational anisotropy along the direction of the applied **E** field. In either case, the resulting orientational anisotropy give rise to an optical birefringence in the sample, which is monitored by the probe pulse. A pulsed probe beam, in conjunction with two delay lines (0–600 ps and 0–30 ns), was used for monitoring decays up to 30 ns. For longer decay times, following pulsed excitation, a cw probe beam and a fast digitizer are employed to measure the decay.

An in-house built solid-state laser system was used to generate the optical pulses. The system consisted of a Ti:sapphire oscillator that was regeneratively amplified. The amplifier was pumped by a Q-switched, intracavity double Nd:YAG laser. The system produced 400 μJ pulses (prior to compression) at a repetition rate of 5 kHz, centered at 800 nm. An adjustable grating compressor permitted pulse durations of <80 fs to 2 ps (FWHM) to be obtained. The longer pulses are achieved by incomplete compression. In addition, bypassing the grating compressor entirely yields pulses of ~100 ps FWHM. The partially compressed and uncompressed pulses are chirped. The use of chirped pulses does not interfere with the production or detection of the optical Kerr effect because it is a nonresonant experiment. The shortest pulses were used to resolve fastest time-scale data. Better signal to noise was obtained at long times by using longer pulses with greater average power. The CW probe was obtained from a commercial diode laser, centered at 635 nm, with an average output power of 15 mW.

Optical heterodyne detection,[32,33] employed the addition of a slightly rotated quarter wave plate to the probe beams, resulting in improved signal to noise ratios and a linear signal in the third-order dielectric susceptibility. Data were collected over 4 distinct time ranges: 0–20 ps using 70 fs pulses and a 0.1 μm stepper motor delay line; 3–600 ps using 1 ps pulses and a 0.1 μm stepper motor delay line; 0.1–30 ns using 100 ps pulses and a quadruple passed long delay line; and 10–200 ns using 100 ps pump pulses, a CW probe, and a fast digitizer. The significant overlap between all four time ranges permitted the data sets to be merged by multiplication of data amplitude until decays were coincident. Care was taken to insure data overlap between differing time scales was excellent.

Sample cuvettes (1 cm optical length) were cleaned on a distillation apparatus to remove dust and other contaminates. DBT, obtained from Aldrich, was purified by fractional vacuum distillation and sealed in the optical cuvettes while still attached to distillation apparatus. Temperature control was obtained via a constant flow cryostat, with temperature stability of ±0.1 K.

III. IDEAL MODE COUPLING THEORY

Ideal MCT for supercooled liquids predicts a multistep relaxation process for the dynamics and a kinetic transition that is predicted to occur at the MCT critical temperature, T_c, which is usually located at approximately 20% above T_g. While MCT makes predictions concerning the density–density correlation function $[\phi_q(t)]$, many experimental

methods, e.g., dielectric spectroscopy[40] and dynamic light scattering,[41] probe orientational relaxation. It is assumed that the time dependence of any correlation function that is coupled to the density is similar in nature to the time dependence of the density–density correlation function.[9,42] MCT is derived for simple liquids (spheres), which do not have orientational degrees of freedom. To investigate the effect of orientational degrees of freedom, molecular-dynamics simulations involving translational and orientational degrees of freedom have been performed.[29,30] In general, the results of the simulations are consistent with MCT for both translational and orientational correlation functions.[30] In this work, it is assumed that results derived for the time dependence of the density–density correlation function can be applied to the polarizability-polarizability correlation function (orientational relaxation), which underlies the HD-OKE measurements.

Within the multistep relaxation scenario of ideal MCT, two power laws, with power law exponents a and b, are discussed when the theory is considered in first order. Near the ideal mode coupling transition temperature T_c, the long time tail of the very short time dynamics is characterized, in first order, by the critical decay law,[6,9]

$$\phi_q(t) = f_q^c + |\sigma|^{1/2} h_q \left(\frac{t}{t_\sigma}\right)^{-a}. \tag{1}$$

f_q^c denotes the critical Debye–Waller factor,[43] h_q the critical amplitude, and

$$t_\sigma = t_0 |\sigma|^{-1/2a} \tag{2a}$$

a rescaling time determined by a microscopic time t_0. More generally,

$$t_\sigma \propto |\sigma|^{-1/2a}, \tag{2b}$$

and the temperature dependence is introduced by

$$\sigma = (T_c - T)/T_c. \tag{3}$$

MCT predicts that the exponent, a, falls in the range $0 \leqslant a \leqslant 0.395$, and it is independent of the actual observable that is coupled to the density. The initial decay of ϕ_q from the plateau value f_q^c is described in first order by another power law, the von Schweidler Law,

$$\phi_q(t) = f_q^c - |\sigma|^{1/2} h_q B \left(\frac{t}{t_\sigma}\right)^{b}, \quad B > 0. \tag{4}$$

The von Schweidler power law describes the onset of the structural relaxation, which is approximately exponential at long times. Another time scale is described by τ_α, with

$$\tau_\alpha \propto |\sigma|^{-\gamma}, \quad \gamma = \frac{1}{2a} + \frac{1}{2b}. \tag{5}$$

τ_α characterizes the longest time scale of complete structural relaxation, α relaxation. Both time scales, t_σ and τ_α, follow characteristic scaling laws, which describe the slowing down of dynamics as the temperature is reduced.

One prediction of MCT is the relationship between the two power law exponents a and b,

$$\lambda = \frac{\Gamma^2(1-a)}{\Gamma(1-2a)} = \frac{\Gamma^2(1+b)}{\Gamma(1+2b)}, \tag{6}$$

where Γ denotes the complete gamma function. The power laws given in Eqs. (1) and (4) are the leading terms of the power law expansions[36,44] of the correlation function,[45] which approximate the full, numerical solutions to the kinetic equations arising in MCT. Using the higher order terms,[36] the behavior between the limiting power laws given in Eqs. (1) and (4) can be calculated with 1% accuracy.[36] The extended forms of Eqs. (1) and (4) are, for times $t_0 < t \leqslant t_\sigma$,

$$\phi_q(t) = f_q^c + h_q |\sigma|^{1/2} [(t/t_\sigma)^{-a} - A_1 (t/t_\sigma)^{a} + A_2 (t/t_\sigma)^{3a} - A_3 (t/t_\sigma)^{5a} + \cdots], \tag{7}$$

and for $t_\sigma < t \leqslant \tau_\alpha$,

$$\phi_q(t) = f_q^c + h_q |\sigma|^{1/2} [-B(t/t_\sigma)^{b} + (B_1/B)(t/t_\sigma)^{-b} + \cdots]. \tag{8}$$

Taking the higher order terms in the expansion of the density–density correlation function into account, theoretical predictions can be compared to experimental data over a wide time window.

IV. RESULTS AND DISCUSSION

An OHD-OKE data set for DBP at 234.0 K is displayed in Fig. 1 on a log plot. At very short time (<500 fs), the data are dominated by the electronic polarization, which tracks the pulse duration. In this data set, to suppress the excitation of intramolecular vibrational modes, which produce oscillation on the decay out to several ps,[1,11] the pulse was lengthened to 115 fs. Two power law regions are distinguishable by the linear appearance on a log plot, the first spanning a range of approximately ~10 ps to ~200 ps and the second a range of ~300 ps to ~2000 ps. As discussed below, the second power law corresponds to the von Schweidler region and the onset of structural relaxation. Following the von Schweidler power law ($t > \sim 10$ ns), the data decay approximately as an exponential. As discussed below, the long time scale portion of the data, which corresponds to the α relaxation, is fit with a function that incorporates both the power law and an exponential.

While the details of the data change with temperature, the basic appearance of the decay curves are the same at all temperatures, even below T_c. This can be seen in Fig. 2, where data sets are displayed for the range of temperatures studied, 220–297.7 K. For this plot, all data sets were normalized to one at $t = 0$. The top curve is the highest temperature, and the bottom curve is the lowest temperature. The temperatures for all curves are given in the figure caption. One qualitative feature that does change with temperature can be seen at ~2 ps. At the lowest three temperatures, which are at or below T_c, a distinct peak appears in the data. This peak, which will be discussed further below, is not evident at the highest temperatures. Also shown in the figure is a dashed line that corresponds to a power law of $t^{-2/3}$. This line is intended as an aid to the eye. It can be seen that the

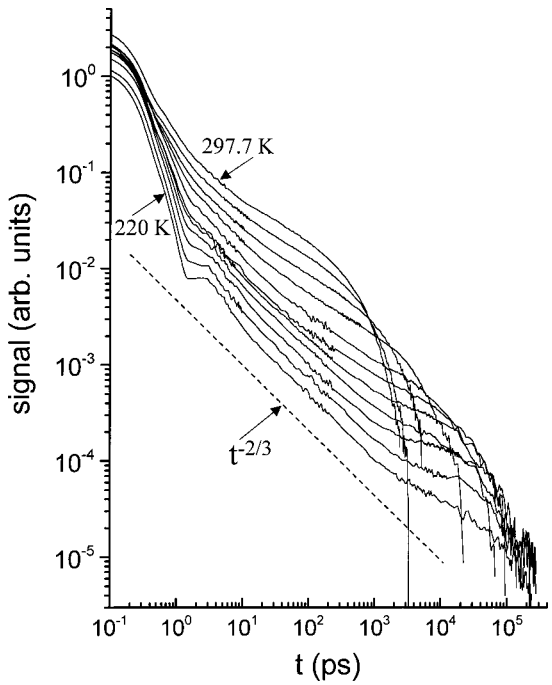

FIG. 2. Complete OHD-OKE data sets are displayed for DBP at temperatures (from bottom to top) 220, 223, 226, 230, 234, 238, 245, 260, 275, 290, and 297.7 K. The data are shown on a log plot and are normalized at $t=0$. A dashed line, corresponding to a power law, $t^{-2/3}$ is shown as a guide to the eye.

lowest temperature decay (220 K) has a power law portion that is parallel to the line from ~10 ps to ~1 ns.

Portions of data spanning the temperatures 220–297.7 K are displayed in Fig. 3. (The temperature for each curve is given in figure caption 2.) The curves have been displaced along the vertical axis for clarity of presentation. Also shown in the figure is a dashed line running through each data set. All the dashed lines have the same slope. The dashed lines correspond to a power law with exponent, $p_1=-0.43$. This value was obtained from the average of fits to the data in the region just before the onset of the long time approximately exponential decay, that is, the von Schweidler region. As can be seen in Fig. 3, each curve has a portion with essentially the same power law decay, independent of temperature. As the temperature is decreased, the onset of the von Schweidler power law moves to longer time.

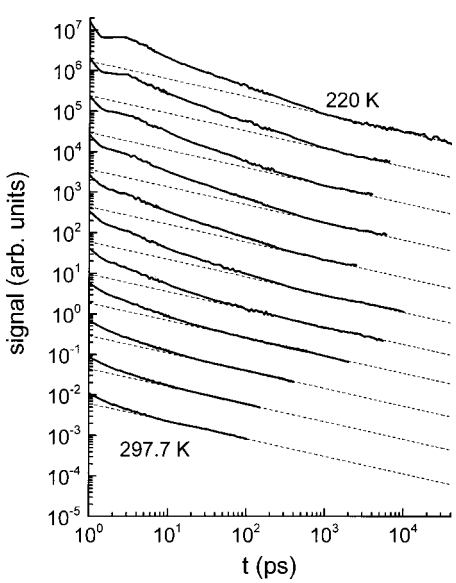

FIG. 3. Portions of DBP data starting at 1 ps and ending at the onset of exponential-like relaxation are compared to a power law with exponent −0.43. For each curve, the long time portion of the displayed data decays as a power law. The power law is temperature independent and corresponds to the von Schweidler power law. Temperatures displayed are (from top to bottom) 220, 223, 226, 230, 234, 238, 245, 260, 275, 290, and 297.7 K. The data sets are offset on the vertical axis for clarity of presentation.

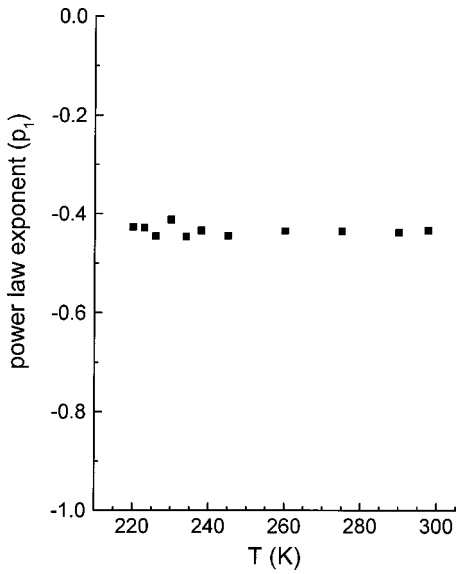

FIG. 4. Power law exponents, p_1, obtained from fits to power law portions of the data displayed in Fig. 3. Within experimental error, the power law exponent is temperature independent and has an average value of −0.43. The von Schweidler power law exponent, b, is related to power law exponent p_1 by $b=p_1+1=0.57$.

Figure 4 displays the temperature dependence of the power law exponent obtained from fits to a single power law for the von Schweidler region at temperatures 220–297.7 K. As can be seen, within experimental error, the power law exponent, p_1, is temperature independent. The average value is −0.43. Since the experiment measures the derivative of the polarizability–polarizability (orientational) correlation function, which is assumed to have the same time dependence as the density–density correlation function, which is calculated in MCT, the actual von Schweidler power law exponent is $b=p_1+1=0.57$. From Eq. (6), this corresponds to $\lambda=0.74$ and a critical decay power law exponent, $a=0.31$. MCT predicts a temperature independent value for b and a value of a that falls in the range $0\leqslant a\leqslant 0.395$.

At times longer than the von Schweidler region, the remaining structural relaxation, α-relaxation, occurs. This region has been observed with a variety of experimental techniques.[12,46,47] In the time domain, the α relaxation is usually fit to a stretched exponential, $\exp(-t/\tau_\alpha)^{-\beta}$.[12,46,47] In the frequency domain, a Cole–Davidson distribution is often used to model the corresponding peak in the susceptibility.[23] The OHD-OKE measures the derivative of the correlation function. The derivative of a stretched exponential is propor-

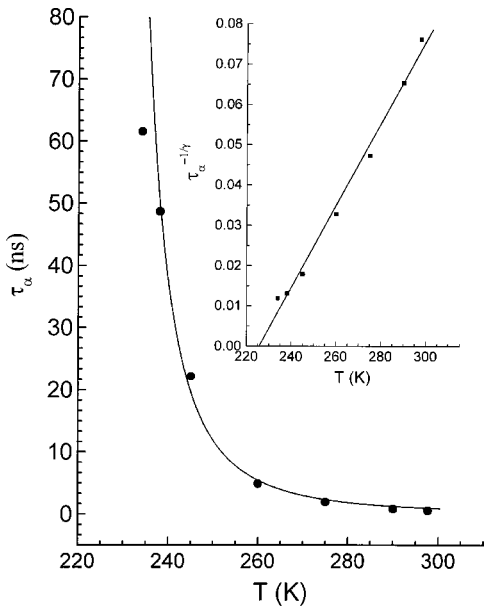

FIG. 5. The α relaxation decay time, τ_α, obtained by fitting the function given in Eq. (9) to the long time portion of the data, is plotted vs temperature. The inset is the corresponding rectification diagram. The points fall on a line as predicted by the MCT scaling relation, Eq. (5). The *x*-intercept of the line yields $T_c = 226 \pm 2$ K. The curve through the data in the main part of the figure is calculated using Eq. (5). There are no adjustable parameters other than a multiplicative amplitude factor that does not influence the shape of the curve.

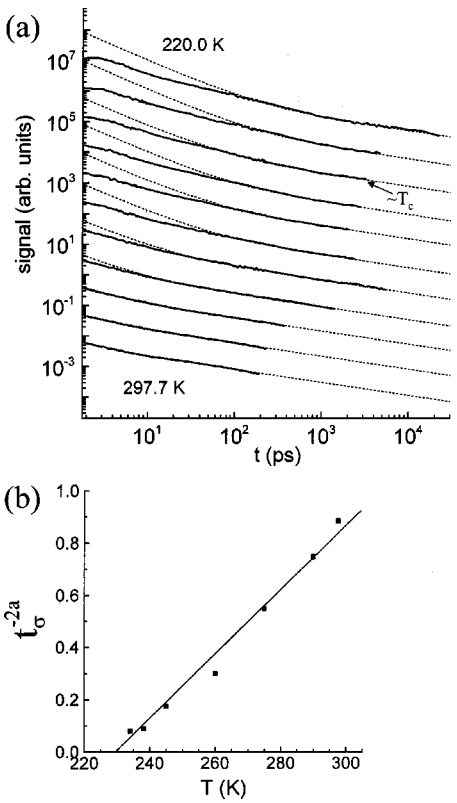

FIG. 6. (a) DBP data compared to MCT master curve calculations [obtained from Eqs. (7) and (8)], using $\lambda = 0.74$ [obtained from Eq. (6) and the von Schweidler power law exponent, (0.57) from Fig. 4]. Agreement between the data and theory is very good at the highest temperatures, but the data and the master curve calculations show substantial differences for $t < 100$ ps at lower temperatures. (b) The rectification diagram based on MCT scaling relationship given in Eq. (2b). The points are predicted to fall on a line with the intercept giving a value of T_c. The fit to the data yields $T_c = 229 \pm 2$ K.

tional to the product of a power law and another stretched exponential,

$$\propto t^{\beta-1} e^{-(t/\tau_\alpha)^\beta}.$$

A simpler function has been found to work well in the analysis of OHD-OKE data.[11] The function is

$$S(t) \propto t^p e^{-t/\tau_\alpha}. \tag{9}$$

Equation (9) is the time derivative of the long time (subscript L) portion of the correlation function, $\Phi_L(t)$. The correlation function is found by integrating the right-hand side of Eq. (9) to give $f(t)$, determining the constant of integration by the boundary condition that $\Phi_L(t) \to 0$ as $t \to \infty$, and normalizing the correlation function at $t = 0-1$. The result is

$$\Phi_L(t) = 1 - f'(t), \tag{10}$$

where $f'(t)$ is $f(t)$ multiplied by the $t=0$ normalization constant. $f'(t)$ is zero at $t=0$ and 1 at $t=\infty$. $f(t)$ is the incomplete gamma function,

$$f(t) = \gamma(p+1, t/\tau_\alpha). \tag{11}$$

$\Phi_L(t)$ corresponds to the correlation function for the long time portion of the decay.

The DBP α relaxation data are fit with Eq. (9) using a value of p that did not depend systematically on temperature. The value of p is not p_1 found in Fig. 4 because p was obtained by fitting out to the longest times, and the exponential has a significant influence on it. The average value of p is -0.28. Fitting with Eq. (9) leads to a well-defined relaxation time τ_α. Figure 5 displays values of τ_α as a function of temperature. The inset displays the data on a ''rectification diagram.'' Within experimental error, the points fall on a line as predicted by the MCT scaling relation [Eq. (5)]. Extrapolation of the line to zero yields the value of $T_c = 226 \pm 2$ K. The curve through the data in the main portion of the figure was generated using Eq. (5) with $a = 0.309$, which is obtained from the von Schweidler b exponent, and $T_c = 226$ K. Other than a multiplicative constant, which does not change the shape of the curve, there are no adjustable parameters. For a temperature independent power law exponent p, the functional form (stretching) of the α process is temperature independent. The time scaling of the correlation function $\Phi_L(t)$ for different values of τ_α can be demonstrated analytically. Therefore, MCT does a very good job of describing the data in both the von Schweidler and α relaxation regimes (moderate to long time scales).

In Fig. 6(a) the experimental data are compared to the full master curves [Eqs. (7) and (8)] (Refs. 36, 44) predicted by MCT. The master curves in Fig. 6(a) utilize the λ parameter 0.74 obtained from the b exponent of the von Schweidler power law. Figure 6(a) is a direct comparison of the data to the master curves. Figure 6(b) is the corresponding rectification diagram based on the scaling law given in Eq. (2b). As predicted by MCT, the points fall on a line. The extrapolation of the line to zero gives a value of $T_c = 229 \pm 2$ K. Within

experimental error, the value of T_c is consistent with the value obtained from the α relaxation rectification diagram in Fig. 5. The average value is 227.5 ± 3 K, which is in accord with previous measurements of 221 K (Refs. 48, 49) and 233 K.[50]

The comparisons of the master curves to the data in Fig. 6(a) show excellent agreement at the three highest temperatures. However, as the temperature approaches T_c, there is an increasing deviation from the master curve predictions. The deviations increase in magnitude and begin at increasingly earlier times as the temperature is decreased toward T_c. Calculation of the master curves for various values of λ about 0.74 only made the disagreement with the data worse. As T_c is approached, the data and the master curve begin to deviate at $\sim$100 ps. In all cases, the deviations are such that the data are much flatter than the master curve calculations at short times. There is no abrupt change in the nature of the curves at and below T_c.

The deviations between the DBP data and the master curves are in stark contrast to previous results on Salol using the identical experiments,[1] where essentially perfect agreement between the data with the master curves was found on all time scales from high temperature down to T_c. In OTP, also studied with the same experiments,[11] the agreement between the data and the master curves was also excellent, but not as good as for salol. In OTP, small deviations are seen for times $<$10 ps as T_c is approached. The extent of the disagreement between the DBP data and the master curves is so much greater than in either salol or OTP that it suggests that there is something fundamentally different in the nature of DBP compared to salol and OTP. Additional differences are discussed below.

An additional peak at approximately 2.5 ps can be seen in the data at T approaches and then goes below T_c. The peak is evident in Figs. 3 and 6, which are log plots. Figure 7 displays short time data from 0 to 5 ps at temperatures 205, 210, 215, 220, and 230 K (top to bottom) on a linear plot. At 230 K, which is just above T_c, the peak is not visible. As the temperature is decreased, the peak becomes very pronounced. It also appears that as T decreases, the peak moves somewhat to longer time. A possible explanation for the peak is that it is a boson peak. A similar phenomenon has been observed in experiments on salol in the time domain.[1] However, in DBP, in contrast to salol, the peak only appears at low temperatures, and it is much more prominent. In salol, at $\sim$0.5 THz, an enhancement in the susceptibility can be found, which is attributed to the boson peak.[51–54] In specific heat measurements, the boson peak shows up as an excess contribution.[55] Several explanations for the boson peak have been proposed,[56–58] however, there is not complete agreement on the microscopic origin of the boson peak.

As can be seen in Fig. 6, the DBP data are much flatter than the decay predicted by MCT. On time scales shorter than the von Schweidler regime, the data has the appearance of a power law. In Fig. 2, a line representing a $t^{-2/3}$ power law can be seen to parallel the low temperature data over a wide range of times. At higher temperatures, the ''intermediate'' power law spans narrower time range, but it can still be observed. This is not the short time critical power law decay

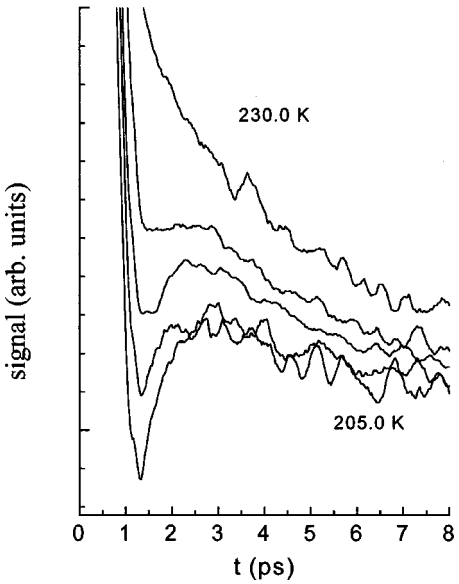

FIG. 7. Fast decay portions (0–8 ps) of DBP data at temperatures (top to bottom) 205, 210, 215, 220, and 230 K are displayed on a linear plot. A peak in the data at $\sim$2.5 ps is clearly visible as the temperature is reduced below 230 K.

described by the exponent a. It occurs on times longer than the critical decay but shorter than the von Schweidler power law. Previous OHD-OKE experiments on salol and OTP (Refs. 1, 2, 11) also observed a power law region located between the critical decay and von Schweidler regions. This intermediate power law region is not predicted by mode coupling theory. Both salol and OTP displayed similar temperature dependences for the intermediate power law. The power law exponent value varies from ~ -0.6 at $T \sim 20\%$ above T_c, and it decreases to ~ -1 close to and just below T_c.[11]

Figure 8 displays the intermediate power law exponent for DBP from temperatures above the melting point to below

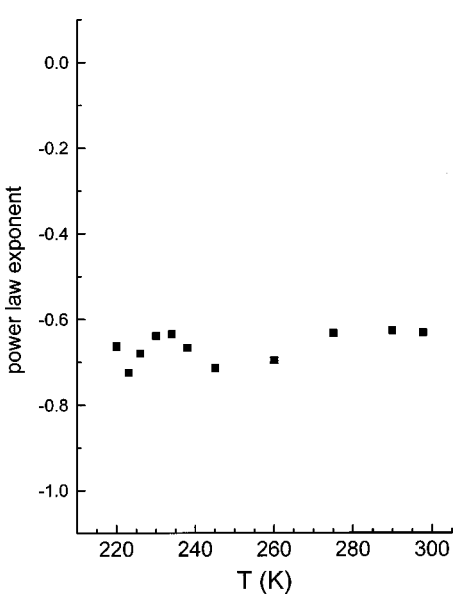

FIG. 8. Intermediate power law exponent plotted vs temperature. Within experimental uncertainty, the intermediate power law exponent is temperature independent.

T_c. As the temperature is decreased, the range spanned by the power law increases. At the highest temperatures in covers on about a decade, from ~2 ps to ~20 ps. At 220 K, the power law spans two decades from ~10 ps to 1 ns (see Fig. 2). As can be seen in Fig. 8, within experimental uncertainty, the power law exponent is temperature independent. The average value obtained for the intermediate power law exponent is -0.66. The lack of temperature dependence of the intermediate power law exponent is qualitatively different from the salol and OTP experimental results.[11]

Ideal MCT describes the salol data down to T_c virtually perfectly,[1,2] and it describes the OTP data down to T_c very well.[11] An important question is whether the agreement between MCT and the salol and OTP data is just a fluke or is there something basically different about DBP that causes it not to be consistent with MCT? The difference between DBP and the other two liquids may be related to their fragility.[59,60] By one measure of fragility, the *m* value, the difference between the behaviors of the three supercooled liquids does not seem to be caused by their fragility.[35] However, a potentially better measure of the fragility is the ratio T_c/T_g, where T_g is the glass transition temperature.[61,62] The ratio is 1.34 for DBP compared to 1.21 for salol and 1.18 for OTP. For comparison, the ratio for propylene carbonate is 1.14, and for glycerol it is 1.31.[63] Propylene carbonate is considered a very fragile liquid. Salol and OTP are also considered quite fragile. In contrast, glycerol is considered a reasonably strong liquid. Thus, DBP is significantly less fragile than salol and OTP. Therefore, the larger deviations between the DBP experiments and the predictions of the ideal MCT master curve compared to the much smaller deviations for salol and OTP may arise because DBP is a relatively strong liquid. Glycerol might be expected to be a relatively strong liquid because it forms extended hydrogen bonded networks. DBP does not hydrogen bond, but, as discussed below, it may form a type of extended structure that influences its fragility and the form of the short time scale dynamics.

MCT predicts a master curve that is temperature dependent through the temperature dependent time scaling. The DBP data consist of a temperature independent power law at times short compared to the von Schweidler region, which is itself temperature independent. The temperature independent power law is very different from the behaviors of salol and OTP, but it is very similar to recent detailed observations on the temperature dependent orientational dynamics of the isotropic phase of liquid crystals[64,65] and on previous studies of orientational relaxation in liquid crystals.[66,67] The recent studies of three liquid crystals,[64,65] employed the identical experimental methods used here to investigate DBP. At long times, the liquid crystal data decay exponentially. The decay is highly temperature dependent[68] as described by Landau–de Gennes theory.[69,70] As the temperature is reduced toward the isotropic to nematic phase transition, the long time decay slows dramatically. The long time decay is analogous to the α relaxation of supercooled liquids. At short times (tens of ps), the data decay as a power law. Between the short time power law and the long time exponential, there is a nonexponential crossover regime. Recent theory[64] suggests that the crossover region observed in liquid crystals[64] occurs for the same reason as the von Schweidler region of supercooled liquids, that is, stretching of the relaxation at intermediate times. On all time scales, the liquid crystal orientational dynamics arise because of the existence of pseudonematic structures (domains) in the isotropic phase.

In addition to the qualitative features of orientational dynamics in the isotropic phase of liquid crystals that are similar to supercooled liquids, there is one feature that is strikingly similar to DBP in particular. The relatively short time scale power laws observed in three different liquid crystals all have exponents that are temperature independent and the exponents range between -0.63 and -0.75, depending on the liquid crystal.[65] The DBP intermediate power law occurs on the same time scale as the liquid crystal power laws. The DBP intermediate power law is temperature independent and has an exponent of ~ -0.66 (see Fig. 8).

Recall that the experiments on the three liquid crystals and on the three supercooled liquids were all performed with identical techniques. It is interesting to speculate on why the DBP orientational dynamics seem more similar to the dynamics of the isotropic phase of liquid crystals than they are to the dynamics of the fragile supercooled liquids, salol and OTP, and to the predictions of MCT. The molecule DBP, which is the ortho-dibutylester of benzene, has an aromatic end and a hydrocarbon end (see inset Fig. 1). The benzene moiety is highly polarizable. It is next to the two ester groups that will have some dipole moment. Thus, the benzene is highly polarizable and may have an induced dipole moment. In contrast, the hydrocarbon portion of DBP has very low polarizability and is essentially nonpolar. Given these aspects of DBP, it is possible that it has some nanoscopic organization much as liquid crystals have pseudonematic domains in the isotropic phase. If nanoscopic organization exists in DBP, then such organization could be responsible for the relative strength of DBP and have an impact on the orientational dynamics, producing behavior that is similar to that of liquid crystals. Additional experiments on other supercooled liquids that will not have the possibility of nanoscopic organization and ones that form networks are in progress. These experiments will help determine under what circumstances ideal MCT describes the dynamical behavior of supercooled liquids down to T_c.

V. CONCLUDING REMARKS

Optical heterodyne detected optical Kerr effect experiments were performed on the glass forming liquid dibutylphthalate over temperatures that range from well above the melting point to below the critical MCT transition temperature, T_c. Additional data were collected at short time down to temperatures ~20 K below T_c. The time domain techniques used spanned a time range of several hundred fs to hundreds of ns. The data at all temperatures share certain features, namely, two distinct power law regions followed by approximately exponential relaxation at long times.

The experimental results were compared to the predictions of ideal MCT. The longer time portions of the data agree with the predictions of MCT exceedingly well (see Figs. 3–5). As predicted, a temperature independent von Schweidler power law is observed with a temperature inde-

pendent power law exponent. The von Schweidler power law reflects the onset of full structural relaxation. The long time scale α relaxation is highly temperature dependent and obeys the MCT scaling relationship. From the α relaxation rectification diagram, T_c is found to be 226 K. Comparisons of the intermediate through short time scale data to the MCT calculated master curves display some agreement with MCT but also significant disparities. The rectification diagram obtained from the data/master curve analysis obeys the MCT scaling relationship (Fig. 6) and yields a value of $T_c = 229\,\mathrm{K}$, which is within experimental error of T_c determined from the α relaxation rectification diagram. The master curves agree well with the data at the highest temperatures, but show increasingly pronounced deviations at short times ($<$100 ps) as the temperature is decreased toward T_c. The form of the data does not change as the temperature is reduced below T_c. The disagreement of the DBP data with the MCT calculations is very different from the very good agreement found for data taken on salol and OTP with the identical experimental methods[1,2,11] and because by the differences in the fragility of the three liquids.

Another indication of a fundamental difference between the dynamics in DBP and salol/OTP is the nature of the temperature dependence of the decay on intermediate time scales (short compared to the von Schweidler region but longer than a few ps). In all three liquids, the intermediate time scale data can be fit to a power law. This power law is not a component of MCT. In salol and OTP, the intermediate power law is temperature dependent; the decay becomes steeper as the temperature is reduced. Within experimental error, for salol and OTP, when the temperature is scaled by T_c, the intermediate power law has the same temperature dependence for the two liquids, with the exponent varying between -0.6 at high temperature and -1 at $\sim T_c$. DBP displays a temperature independent intermediate power law with exponent ~ -0.66. It was pointed out that the orientational dynamic observed in DBP have a striking resemblance to those observed in the isotropic phase of liquid crystals. Further experiments are being performed on other supercooled liquids to determine under what circumstances ideal MCT gives an accurate description of time and temperature dependence of orientational dynamics in supercooled liquids.

ACKNOWLEDGMENTS

The authors thank Dr. Gerald Hinze, Institut für Physikalische Chemie, Johannes Gutenberg-Universität, Welderweg 15, D-55099 Mainz, for helpful conversations pertaining to this work. This research was supported by the National Science Foundation (DMR-0088942).

[1] G. Hinze, D. D. Brace, S. D. Gottke, and M. D. Fayer, J. Chem. Phys. **113**, 3723 (2000).
[2] G. Hinze, D. D. Brace, S. D. Gottke, and M. D. Fayer, Phys. Rev. Lett. **84**, 2437 (2000).
[3] R. Torre, M. Ricci, P. Bartolini, C. Dreyfus, and R. M. Pick, Philos. Mag. B **79**, 1897 (1999).
[4] G. Hinze and H. Sillescu, J. Chem. Phys. **104**, 314 (1996).
[5] F. Fujara, B. Geil, H. Sillescu, and G. Fleischer, Z. Phys. B: Condens. Matter **88**, 195 (1992).
[6] W. Götze and L. Sjögren, Rep. Prog. Phys. **55**, 241 (1992).
[7] C. A. Angell, J. Phys. Chem. Solids **49**, 863 (1988).
[8] I. Chang and H. Sillescu, J. Phys. Chem. **101**, 8794 (1997).
[9] W. Götze, J. Phys.: Condens. Matter **11**, A1 (1999).
[10] K. L. Ngai, E. Riande, and G. B. Wright, J. Non-Cryst. Solids **172-174**, 1 (1994).
[11] S. D. Gottke, D. D. Brace, G. Hinze, and M. D. Fayer, J. Phys. Chem. B **105**, 238 (2001).
[12] H. Z. Cummins, G. Li, W. Du, Y. H. Hwang, and G. Q. Shen, Prog. Theor. Phys. **126**, 21 (1997).
[13] W. Steffen, A. Patkowski, H. Gläser, G. Meier, and E. W. Fischer, Phys. Rev. E **49**, 2992 (1994).
[14] R. Bergmann, L. Börjesson, L. M. Torell, and A. Fontana, Phys. Rev. B **56**, 11 619 (1997).
[15] V. Krakoviack, C. Alba-Simionesco, and M. Krauzman, J. Chem. Phys. **107**, 3417 (1997).
[16] G. Li, M. Du, A. Sakai, and H. Z. Cummins, Phys. Rev. A **46**, 3343 (1992).
[17] G. Li, W. M. Du, X. K. Chen, and H. Z. Cummins, Phys. Rev. A **45**, 3867 (1992).
[18] A. Tölle, H. Schober, J. Wuttke, and F. Fujara, Phys. Rev. E **56**, 809 (1997).
[19] M. Kiebel, E. Bartsch, O. Debus, F. Fujara, W. Petry, and H. Sillescu, Phys. Rev. B **45**, 10 301 (1992).
[20] W. Petry, E. Bartsch, F. Fujara, M. Kiebel, H. Sillescu, and B. Farago, Z. Phys. B: Condens. Matter **83**, 175 (1991).
[21] J. Wuttke, M. Kiebel, E. Bartsch, F. Fujara, W. Petry, and H. Sillescu, Z. Phys. B: Condens. Matter **91**, 357 (1993).
[22] P. Lunkenheimer, A. Pimenov, M. Dressel, Y. G. Goncharov, R. Böhmer, and A. Loidl, Phys. Rev. Lett. **77**, 318 (1996).
[23] U. Schneider, P. Lunkenheimer, R. Brand, and A. Loidl, Phys. Rev. E **59**, 6924 (1999).
[24] A. Arbe, D. Richter, J. Colmenero, and B. Farago, Phys. Rev. E **54**, 3853 (1996).
[25] M. Giordano, D. Leponini, and M. Tosi, J. Phys.: Condens. Matter **11**, A1 (1999).
[26] R. Torre, P. Bartolini, M. Ricci, and R. M. Pick, Europhys. Lett. **52**, 324 (2000).
[27] S. R. Kudchadkar and J. M. Wiest (1995).
[28] W. Kob and H. C. Anderson, Phys. Rev. E **52**, 4134 (1995).
[29] S. Kämmerer, W. Kob, and R. Schilling, Phys. Rev. E **56**, 5450 (1997).
[30] S. Kämmerer, W. Kob, and R. Schilling, Phys. Rev. E **58**, 2141 (1998).
[31] T. Franosch, M. Fuchs, W. Goetze, M. R. Mayr, and A. P. Singh, Phys. Rev. E **55**, 7153 (1997).
[32] D. McMorrow, W. T. Lotshaw, and G. Kenney-Wallace, IEEE J. Quantum Electron. **24**, 443 (1988).
[33] D. McMorrow and W. T. Lotshaw, J. Phys. Chem. **95**, 10395 (1991).
[34] G. Hinze, R. Francis, and M. D. Fayer, J. Chem. Phys. **111**, 2710 (1999).
[35] D. Huang and G. B. Mckenna, J. Chem. Phys. **114**, 5621 (2001).
[36] W. Götze, J. Phys.: Condens. Matter **2**, 8485 (1990).
[37] A. P. Sokolov, E. Rössler, A. Kisliuk, and D. Quitmann, Phys. Rev. Lett. **71**, 2062 (1993).
[38] S. Ruhman, L. R. Williams, A. G. Joly, B. Kohler, and K. A. Nelson, J. Phys. Chem. **91**, 2237 (1987).
[39] F. W. Deeg and M. D. Fayer, J. Chem. Phys. **91**, 2269 (1989).
[40] C. J. F. Böttcher and P. Bordewijk, *Theory of Electric Polarization* (Elsevier, Amsterdam, 1992).
[41] B. J. Berne and R. Pecora, *Dynamical Light Scattering* (Krieger, Malabar, 1990).
[42] W. Götze and R. Haussmann, Z. Phys. B: Condens. Matter **72**, 403 (1988).
[43] S. W. Lovesey, *Theory of Neutron Scattering from Condensed Matter* (Clarendon, Oxford, 1984).
[44] E. Bartsch, Transport Theory and Statistical Physics **24**, 1125 (1995).
[45] G. Li, G. M. Fuchs, W. M. Du, A. Latz, N. J. Tao, J. Hernandez, W. Götze, and H. Z. Cummins, J. Non-Cryst. Solids **172**, 43 (1994).
[46] M. Fuchs, I. Hofacker, and A. Latz, Phys. Rev. A **45**, 898 (1992).
[47] W. van Megen and S. M. Underwood, Phys. Rev. E **49**, 4206 (1994).
[48] E. Rossler, J. Chem. Phys. **92**, 3725 (1990).
[49] S. A. Dzuba, Z. Phys. B: Condens. Matter **83**, 303 (1991).
[50] J. Wuttke and M. Goldammer (unpublished results).
[51] U. Buchenau, M. Prager, N. Nücker, A. J. Dianoux, N. Ahmad, and W. A. Phillips, Phys. Rev. B **34**, 5665 (1986).
[52] A. P. Sokolov, E. Rössler, A. Kisliuk, M. Soltwisch, and D. Quitmann, Physica A **201**, 67 (1993).
[53] C. Masciovecchio, G. Ruocco, F. Sette, M. Krisch, R. Verbeni, U. Bergmann, and M. Soltwisch, Phys. Rev. Lett. **76**, 3356 (1996).

[54] M. Foret, E. Courtens, R. Vacher, and J.-B. Suck, Phys. Rev. Lett. **77**, 3831 (1996).
[55] R. C. Zeller and R. V. Pohl, Phys. Rev. B **4**, 2029 (1971).
[56] V. G. Karpov, M. I. Klinger, and F. N. Ignat'ev, Sov. Phys. JETP **57**, 439 (1983).
[57] A. P. Sokolov, J. Phys.: Condens. Matter **11**, A213 (1999).
[58] W. Schirmacher, G. Diezemann, and C. Ganter, Phys. Rev. Lett. **81**, 136 (1998).
[59] J. Souletie and D. Bertrand, *Different Universality Classes, From Strong to Fragile, of the Glass and Spin Glass Transitions* (American Institute of Physics, New York, 1992).
[60] C. A. Angell, *Relaxation in Complex Systems* (U.S. Department of Commerce, Washinton, DC, 1985).
[61] V. N. Novikov, E. Rössler, V. K. Malinovsky, and N. V. Surovtsev, Europhys. Lett. **35**, 289 (1996).
[62] C. A. Angell, K. L. Ngai, G. B. McKenna, P. F. McMillan, and S. W. Martin, Appl. Phys. Rev. **88**, 3113 (2000).
[63] R. Richert and C. A. Angell, J. Chem. Phys. **108**, 9016 (1998).
[64] S. D. Gottke, D. D. Brace, H. Cang, B. Bagchi, and M. D. Fayer, J. Chem. Phys. (submitted).
[65] S. D. Gottke, H. Cang, B. Bagchi, and M. D. Fayer, J. Chem. Phys. (in press).
[66] F. W. Deeg, S. R. Greenfield, J. J. Stankus, V. J. Newell, and M. D. Fayer, J. Chem. Phys. **93**, 3503 (1990).
[67] J. J. Stankus, R. Torre, and M. D. Fayer, J. Phys. Chem. **97**, 9478 (1993).
[68] J. J. Stankus, R. Torre, C. D. Marshall, S. R. Greenfield, A. Sengupta, A. Tokmakoff, and M. D. Fayer, Chem. Phys. Lett. **194**, 213 (1992).
[69] P. G. de Gennes, Phys. Lett. A **30**, 454 (1969).
[70] P. G. de Gennes, *The Physics of Liquid Crystals* (Clarendon, Oxford, 1974).